ELSEVIER

Journal of Structural Geology 29 (2007) 1960–1970

JOURNAL OF STRUCTURAL GEOLOGY

www.elsevier.com/locate/jsg

Predicting strain using forward modelling of restored cross-sections: Application to rollover anticlines over listric normal faults

Josep Poblet*,[1], Mayte Bulnes[1]

Departamento de Geología, Universidad de Oviedo, C/Jesús Arias de Velasco s/n, 33005 Oviedo, Spain

Received 31 January 2007; received in revised form 1 August 2007; accepted 10 August 2007
Available online 19 August 2007

Abstract

A strategy to predict strain across geological structures, based on previous techniques, is modified and evaluated, and a practical application is shown. The technique, which employs cross-section restoration combined with kinematic forward modelling, consists of restoring a section, placing circular strain markers on different domains of the restoration, and forward modelling the restored section with strain markers until the present-day stage is reached. The restoration algorithm employed must be also used to forward model the structure. The ellipses in the forward modelled section allow determining the strain state of the structure and may indirectly predict orientation and distribution of minor structures such as small-scale fractures. The forward model may be frozen at different time steps (different growth stages) allowing prediction of both spatial and temporal variation of strain. The method is evaluated through its application to two stages of a clay experiment, that includes strain markers, and its geometry and deformation history are well documented, providing a strong control on the results. To demonstrate the method's potential, it is successfully applied to a depth-converted seismic profile in the Central Sumatra Basin, Indonesia. This allowed us to gain insight into the deformation undergone by rollover anticlines over listric normal faults.

Keywords: Strain; Fracture; Cross-section restoration; Forward modelling; Rollover anticline; Listric normal fault

1. Introduction

A number of procedures have been developed to measure the strain from rock samples. Unfortunately, in many folded/faulted regions suitable strain markers are uncommon, they are not present for all points of interest or they are not accessible because the structures are not exposed (poor surface outcrops, subsurface or offshore structures). This is one of the reasons that motivated the development of strain prediction techniques that do not require collecting rock samples from all over the structure under investigation. Strain of folded/faulted strata may be unravelled in cross-sections, maps or 3D surfaces using curvature analysis of folded surfaces (e.g., Lisle, 1994; Samson and Mallet, 1997; Roberts, 2001), forward modelling (e.g., Thorbjornsen and Dunne, 1997; Bastida et al., 2003; Ormand and Hudleston, 2003; Allmendinger et al., 2004), restoration (e.g., Erickson et al., 2000; Rouby et al., 2000; Dunbar and Cook, 2003), restoration plus forward modelling (e.g., Allmendinger, 1998; Sanders et al., 2004), etc. Here we use a strategy similar to the approaches of Allmendinger (1998) and Sanders et al. (2004), since it employs restoration and kinematic forward modelling to quantify different parameters that characterize the strain undergone by rocks in folded/faulted regions. This technique assumes that present-day sections across structures are retro-deformable and that the restorations may be forward modelled successfully using the same algorithm employed for the restoration. This method enables mapping strain orientations and magnitudes onto the cross-section, which may be used to predict

* Corresponding author. Departamento de Geología, Universidad de Oviedo, C/Jesús Arias de Velasco s/n, 33005 Oviedo, Spain. Tel.: +34 98 510 9548; fax: +34 98 510 3103.
E-mail address: jpoblet@geol.uniovi.es (J. Poblet).
[1] Consolider Team "Topo-Iberia".

0191-8141/$ - see front matter © 2007 Elsevier Ltd. All rights reserved.
doi:10.1016/j.jsg.2007.08.003

orientation and distribution of fractures and other minor structures.

The main goals pursued here are: (1) simplify the procedure presented by previous authors so that it can be used even if specific strain-prediction software is not available, (2) enlarge its capabilities so that it may be applied to 2D sections across any type of structures developed in different tectonic environments, (3) evaluate the method, (4) show a practical application of the method using a section across a natural structure, and (5) provide additional insight about internal deformation in rollover anticlines over listric normal faults.

(1) Unlike the procedures of Allmendinger (1998) and Sanders et al. (2004), the technique described here may supply satisfactory results using solely a structural modelling package that includes both cross-section restoration and forward modelling modules, and there is no need for specific software in which all the steps listed below are implemented. For instance, the strain markers necessary to predict the strain state of the structures and contouring the results may be drawn by hand on the cross-sections if no software is available.

(2) Our technique is different to that from Allmendinger (1998) and Sanders et al. (2004). Whereas Allmendinger's technique is applicable to trishear fault-propagation folds, we use several algorithms employed for restoration of different styles of structures developed in contractional, extensional, etc. regimes. In addition, our technique permits the proper restorations to be forward modelled, without being simplified, and therefore, the strain is predicted on cross-sections identical to the deformed present-day cross-sections. The Sanders et al. (2004) technique requires 3D data, whereas our technique is developed for 2D data.

(3) Evaluating the method requires applying it to an example in which the number of uncertainties inherent to natural examples is minimum and many deformation parameters, such as geometry of the initial and final states, deformation history, and amount and sense of tectonic transport, are well documented. Thus, the method is tested on two published sections across an experimental listric normal fault with an associated hangingwall rollover anticline derived from photographs of different stages of the physical experiment (Dula, 1991). In addition, this clay experiment provides a strong structural control on the strain-prediction technique employed because it includes strain markers.

(4) The predictive capabilities of the method are shown through its application to a geological interpretation of a depth-converted seismic profile across a rollover anticline over a growth listric normal fault in the Central Sumatra Basin, Indonesia (Shaw et al., 1997).

(5) The analysis of both the experimental and the natural example of rollover anticlines over listric normal faults furnished information on the internal deformation undergone by this type of extensional structures.

2. Methodology

The method is based on: (1) restoring the present-day cross-section to its pre-deformational stage; (2) introducing some strain markers on the restoration, and (3) deforming the restored section, together with the strain markers, up to the present-day stage.

(1) Cross-section restoration involves a substantial knowledge of the deformation processes that led to the present-day geometries. Unfortunately, most observable geometries in nature, such as dips of beds and offsets across faults, record mainly aspects of the particle displacement field, and consequently, many assumptions must be made about modes of internal deformation within folds and fault blocks. However, this problem may be partially overcome if several restoration algorithms are employed to restore a cross-section and the results are compared to check which one leads to the most reasonable solutions in terms of attitude of beds, structures and pin/loose lines, amount of displacement along faults, and amount of contraction/extension when this parameter is known (for instance in physical experiments). We must keep in mind that the best algorithm does not necessarily reproduce accurately the deformation mechanisms that operate, but provides the best geometrical approximation, at cross-section scale, of the overall lengthening/shortening of the section; however, displacement may be accommodated along several deformation mechanisms. If growth strata are available, it is advisable to perform sequential restorations and check each restored state. To restore the hangingwall rollovers over listric normal faults analysed here, the following restoration algorithms implemented in the software Geosec 2D (Paradigm Geophysical) were used: layer-parallel shear, fault-parallel shear, inclined antithetic shear, vertical shear and inclined synthetic shear.

(2) Once a geologically possible restoration is obtained, circular strain markers must be included. Since placing strain markers all over the restoration is a time consuming task, we recommend placing them in selected parts of the restored state and interpolating the results. Therefore, the accuracy and scale of deformation one would like to illustrate depends on the amount, distribution, spacing and size of the strain markers.

(3) Subsequently, the restored section including circular strain markers must be forward modelled up to the present-day cross-section using the same algorithm employed to carry out the restoration. The circular strain markers in the restored section remain circular or become ellipses in the forward modelled present-day section and show the strain in different sectors of the section across the structure. The restored cross-sections analysed here, together with the strain markers, were forward modelled using the module fault-slip fold implemented in the software Geosec 2D (Paradigm Geophysical). Several parameters such as orientation and length of the semi-axes of the ellipses, directions of no finite longitudinal strain, amount of bed extension/contraction, etc. can be measured from each strain marker. Apart from isolated values, the resulting strain data may be contoured onto the cross-sections using different methods in order to interpolate deformation features between strain markers. Kriging with a linear variogram is the geostatistical gridding method employed here to interpolate the data measured from each strain marker. This interpolation method attempts to express trends that are

suggested in the data, so that points with extreme values might be connected along a ridge rather than isolated by bull's-eye type contours, and honours data points exactly where the data point coincides with the grid node being interpolated.

It is advisable to estimate the incremental strain by freezing the forward models at specific times. If growth strata are available, we recommend freezing the forward models at a different growth stages, that is, when particular growth beds deposit. This allows a comparison of the change in strain from time step "t" with the strain of the previous time step "t − 1". Comparing the strain in the present-day cross-section with the strain in the undeformed cross-section analyses the finite strain but does not consider the geological history, and therefore, is prone to underestimate the total deformation. This is particularly the case for non-planar fault surfaces with substantial displacement in which parts of the structure may show no deformation at a specific stage, although they were intensely deformed at a previous time step (e.g., Sanderson, 1982; Sanders et al., 2004).

3. Evaluating the method

To evaluate the method, it was applied to two sections across two different stages of deformation of a clay experiment that consisted of a relatively simple rollover anticline over a listric normal fault with no secondary faulting (Fig. 1). Dula (1991) supplied a complete description of the experiment including photographs, the experimental procedure and the modelling materials, and Poblet and Bulnes (2005a,b) analysed bed-length, thickness and area variations along this experiment.

This physical experiment provides a powerful test for the method used here, because the present-day geometry of beds/structures and the magnitude and sense of displacement are well constrained, the deformation history is well documented, and the experiment includes strain markers. This enables us to neglect many uncertainties associated with sections across natural examples such as selection of the cross-section lines, dip and position of the pin/loose lines, variations of bed length, bed thickness and/or cross-sectional area during deformation, and geological interpretation (dip and position of beds and structures, depth to detachment, etc.) (e.g., Bulnes and Poblet, 1999), and therefore, the imbalances must be attributed to the modelling algorithms employed. This experiment should allow us to test whether the restoration/forward modelling algorithms that supply correct magnitudes of extension and provide geologically reasonable geometries of beds, faults and pin/loose lines also remove the strain. If so, the ellipses in the present-day cross-sections should retrodeform to their original un-deformed circular shape in the restored sections obtained. The more circular the shape of the restored strain markers, the more successful the strategy. The main disadvantage of using a physical experiment to check the methodology is that it is unclear to what extent it models adequately natural deformation conditions due to scaling problems (rock strength, strain rates, experiment dimensions) and boundary conditions (Withjack et al., 1995).

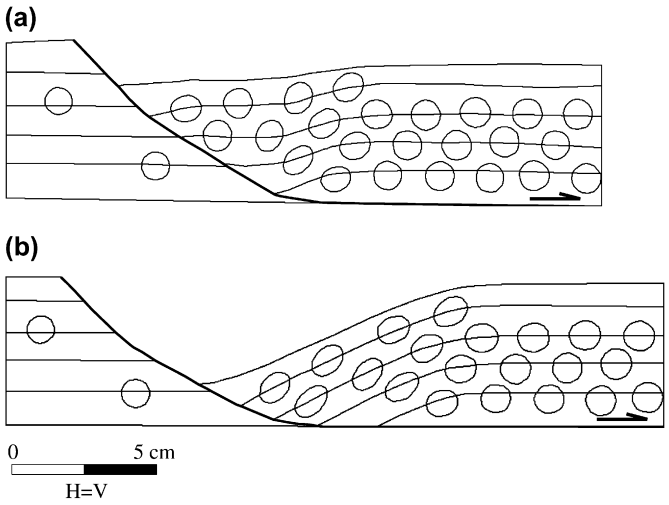

Fig. 1. Line drawings of two sections across a rollover anticline over a listric normal fault derived from two photographs of a clay experiment showing two different stages after (a) 2 cm and (b) 6 cm of total horizontal extension (modified from Dula, 1991).

Instead of applying the full technique described above, consisting of three steps, the occurrence of strain markers in the physical experiment should allow us to evaluate the method by applying only step number one. Thus, there is no need to include circular strain markers in the restored cross-section (step 2) and to forward model the restoration including the circular strain markers to visualize their final shape (step 3). We decided not to apply the full methodology in this case because it is statistically simpler and faster to check whether the restored strain markers are circles than comparing the actual strain ellipses displayed in the experiment photographs with forward modelled strain ellipses.

A number of restorations of the sections together with strain markers, using different algorithms, were carried out but only the most representative ones are shown. Since the footwall and the fault remained undeformed during the whole experiment, the hangingwall beds must adapt to the fault surface (Fig. 2). The reference horizon employed to carry out the restorations was the third one numbering them from top to bottom, except for the fault-parallel shear restoration in which the top horizon was used. The two uppermost beds are thinner in the footwall than in the hangingwall; however, it is likely that this thickness variation is not due to deformation (see the perfect circular shape of the strain markers in the distal part of the hangingwall) (Fig. 1).

The geometry of the beds is geologically reasonable in the restorations using layer-parallel shear, fault-parallel shear, vertical shear and 85° dipping antithetic shear (Fig. 2); however, the last one produces the best results (Fig. 2d and j). This algorithm removes the heave/throw along faults for most beds, provides correct amounts of horizontal extension, creates realistic geometries of the restored hangingwalls and results in vertical loose lines. The restorations obtained are not perfect (for instance, the cut-off points of beds different from the reference bed do not match accurately) because the algorithms

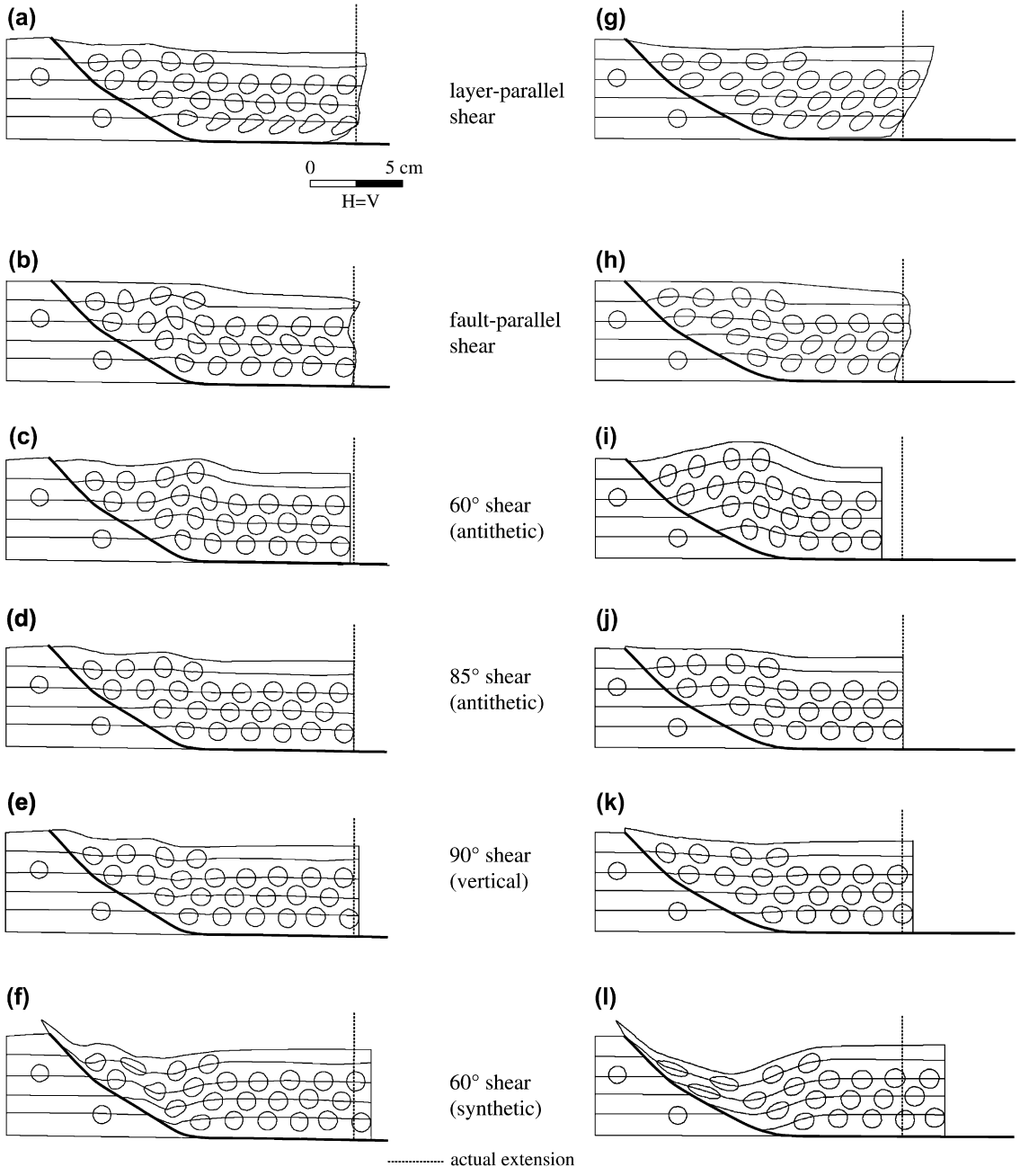

Fig. 2. Restorations of the sections across the experimental rollover anticline over a listric normal fault shown in Fig. 1a (a–f) and in Fig. 1b (g–l), employing: (a,g) layer-parallel shear, (b,h) fault-parallel shear, (c,i) 60° dipping antithetic shear, (d,j) 85° dipping antithetic shear, (e,k) 90° dipping shear (i.e., vertical shear), and (f,l) 60° dipping synthetic shear.

are unable to simulate natural deformation conditions exactly. In addition, the restorations using 85° dipping antithetic shear are the only ones in which most of the strain markers become almost circles in the restored state indicating that almost the whole deformation was removed. Only a few strain markers remain slightly elliptical in the restorations and their position coincides with some irregularities in the beds' shape (Fig. 2d and j). Thus, the mean of ellipticity of the strain markers located above the footwall ramp for both stages of the experiment restored using 85° dipping antithetic shear is 1.15 (close to the mean of ellipticity of undeformed, circular strain markers which is 1) and is 0.05–0.29 less than the mean of the ellipticity calculated in the restorations using other algorithms. This is a good test of the method for this particular example; it indicates that if we had used this algorithm to forward model the physical experiment restoration in order to predict the magnitudes and orientations of strain, the predicted results would be consistent with its actual internal deformation. In other words, substituting the strain markers by perfect circular strain markers in the physical experiment restorations obtained using 85° dipping antithetic shear, and inverting the restoration, should produce present-day state cross-sections with geometry and strain markers' shape similar to that of the sections displayed in Fig. 1.

4. Strain prediction in a depth-converted seismic profile across a natural example

As an application of the technique to a natural example, the geological interpretation of a well imaged depth-converted seismic profile across a growth fault in the Central Sumatra Basin, Indonesia (Shaw et al., 1997) was used (Fig. 3). It consists of a simple rollover fold with no secondary faulting developed over a listric normal fault. From bottom to top, the lowermost four horizons used for modelling purposes are (Fig. 3): the top of the pre-growth beds (top of pre-Tertiary basement), and the top of three Oligocene growth beds of lacustrine, fluvial and marine origin (Shaw et al., 1997). Beds were originally deposited with a palaeodepositional slope around 3° toward the master fault (Shaw et al., 1997).

Before determining strain patterns, several restoration algorithms were tested on the example but only a selection of some restored sections is shown in Fig. 4. The cross-section was sequentially restored using the top of different growth strata as reference horizons for each restoration stage. The restorations performed assume that the onlapping growth beds filled in all the space available, so that once they sedimented the depositional surface was flat and no positive/negative topography/bathymetry existed (“fill to the top” approach according to Masaferro et al., 2002 amongst others).

In contrast to the experimental example analysed in the previous section, this is a natural example and the undeformed stage is unknown, therefore, the geometry of both the hangingwall beds and the loose line is the parameter analysed to choose the best restoration algorithm. The geometry of beds is geologically reasonable in the different restored stages constructed using layer-parallel shear, and 60° and 65° dipping antithetic shear; however, 65° dipping antithetic shear provides the best results (Fig. 4c). The application of the method requires a number of circular strain markers to be included in the total restoration obtained using 65° dipping antithetic shear. The restored cross-section, together with the circular strain markers, was forward modelled using the same algorithm up to the present-day state (Fig. 5). The forward models were frozen at different growth stages in order to consider not only the deformation recorded by the strain markers in the present-day cross-section but the strain accumulated during each increment of growth, that is, the strain history. The ratio between the semi-axes of the ellipses (ellipticity or amount of deformation), the amount of layer parallel extension, the orientation of the maximum elongation, and the orientation of the lines of no finite longitudinal strain were measured from each strain ellipse in the three different growth stages and in the present-day cross-section. Only the results obtained for the present-day cross-section are shown (Fig. 6). The maximum strain attains values of ellipticity greater than 1.60 along an elongated band that has an approximately 50° antithetic dip and runs from the lower part of the fault ramp upwards (Fig. 6a). There is another large elongated band with values of ellipticity greater than 1.20 with an antithetic dip of about 65°, in the region close to the boundary between the hangingwall portion solely translated above the detachment and that rotated and translated. This band is approximately parallel to the axial surface that separates both hangingwall regions. The layer-parallel strain shows a similar distribution to that of the ellipticity with maximum values of about 0.16 to the right of the synclinal hinge where growth beds change their dip from antithetic to synthetic (Fig. 6b). Beds display shallow to moderate antithetic dips in most regions of the present-day cross-section and in these areas the maximum elongation is approximately subparallel to bedding (Fig. 6c); however, close to the upper part of the fault ramp, where growth beds exhibit subhorizontal or synthetic shallow dips, the maximum elongation has a synthetic dip of about 70°. One direction of no finite longitudinal strain has a constant antithetic dip of 65° because the lengths of lines parallel to the shear surfaces employed to restore and forward model the structure are conserved (Fig. 6d). The other direction of no finite longitudinal strain exhibits synthetic moderate dips, except for the hinge of a small syncline delineated by growth beds with antithetic dips in one limb and synthetic in the other limb, in which the direction of no finite longitudinal strain dips steeply.

The variation of these parameters with time, that is, the variation of the maximum elongation orientation, the variation of the orientation of the lines of no finite longitudinal strain, the

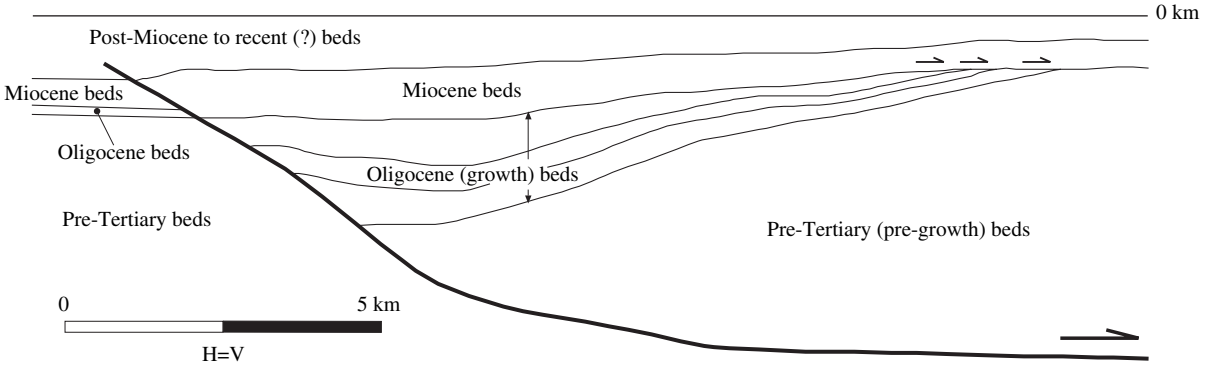

Fig. 3. Line drawing of a section across a growth rollover anticline over a listric normal fault in the Central Sumatra Basin, Indonesia derived from the geological interpretation of a depth-converted seismic profile (modified from Shaw et al., 1997). The small arrows located above the tops of the growth beds indicate onlap positions over older beds.

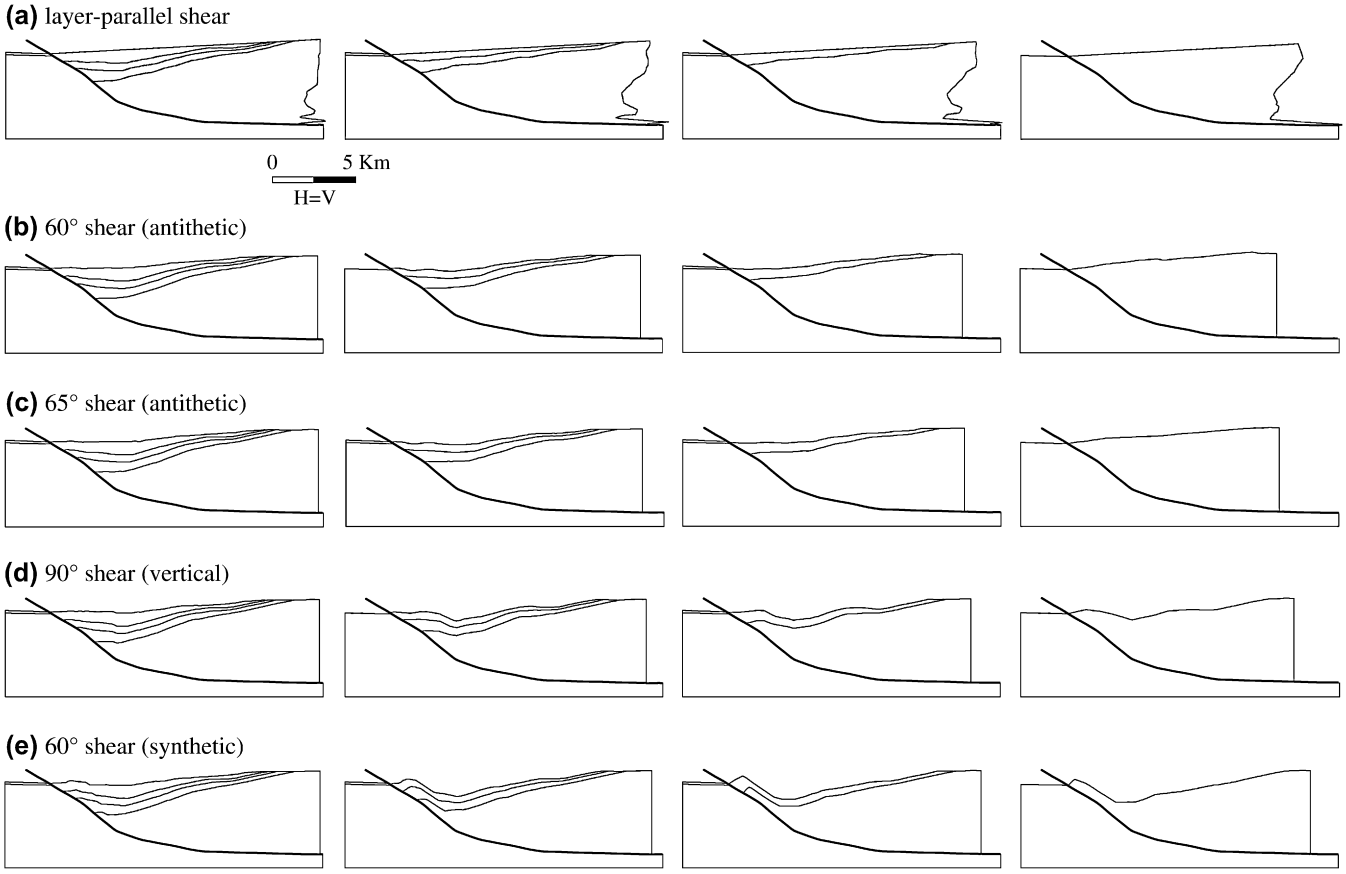

Fig. 4. Sequential restoration of the section across the growth rollover anticline over a listric normal fault in the Central Sumatra Basin, Indonesia shown in Fig. 3 employing: (a) layer-parallel shear, (b) 60° dipping antithetic shear, (c) 65° dipping antithetic shear, (d) 90° dipping shear (i.e., vertical shear) and (e) 60° dipping synthetic shear. The regional datum is inclined around 3° toward the left. Restorations to the top of the uppermost Oligocene growth bed are placed in the left side of the figure, whereas restorations to the top of the pre-Tertiary pre-growth beds are located in the right side of the figure, that is, the age of the restored sections increases from left to right.

incremental ellipticity, the incremental layer parallel extension and the velocity of ellipticity variation (velocity of deformation), were estimated by combining data from the different growth stages and the present-day cross-section (Fig. 7). The incremental ellipticity and the incremental layer parallel extension were estimated as the addition of variations undergone during the different growth stages. The variation of the maximum elongation orientation and the variation of the orientation of the lines of no finite longitudinal strain are displayed as the superposition of orientations obtained from different growth stages. The velocity of ellipticity variation was calculated as the slope of the best-fit function that fits the ellipticity data measured in the different growth stages versus time assuming that the best-fit function is a linear function. The age of the growth beds is needed to estimate velocities. Since no accurate data on the absolute age of each growth bed are available, the sedimentation rate in the depocentres was assumed to remain constant for each growth bed and this allowed us to use bed thickness instead of time.

The contours of incremental ellipticity and incremental longitudinal strain, and the orientation of the maximum extension and directions of no finite longitudinal strain during different growth stages are very similar to those of the present-day cross-section (Fig. 7a–d). The contours of variation of ellipticity with time are similar to those of ellipticity for the present-day cross-section and incremental ellipticity, indicating that the deformation was more rapid in those areas with greater final amounts of deformation (Fig. 7e).

5. Discussion

To apply the methodology presented, the choice of the appropriate restoration algorithm is crucial because different algorithms produce different beds' and faults' configuration, different amounts of extension/contraction and different strain architectures (Fig. 8) (e.g., Bulnes and McClay, 1999). Thus, for the same fault geometry and displacement on the fault but different rollover shape, the ellipticity of the strain markers is similar when 70° dipping antithetic or vertical shear is used, it is slightly lesser when 70° dipping synthetic shear is employed, and it decreases if layer-parallel shear is used (left column of Fig. 8). For the same rollover geometry and displacement on the fault but different fault shape, the ellipticity is similar when 70° dipping antithetic or vertical shear is used, it is slightly greater when 70° dipping synthetic shear is employed, and it increases close to the master fault when

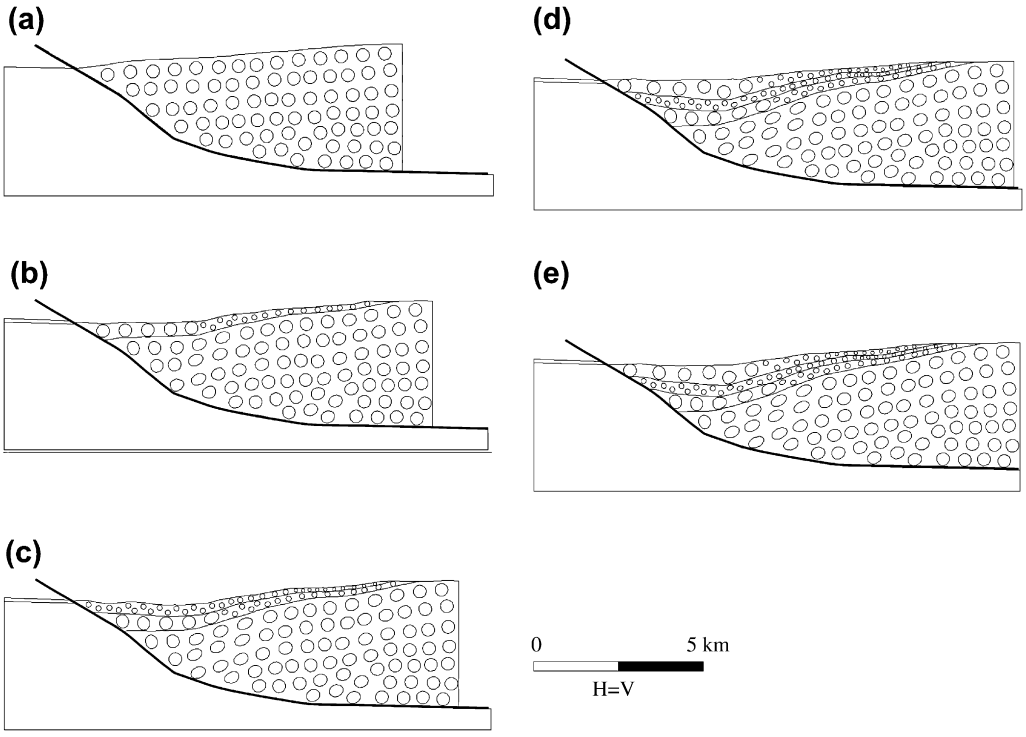

Fig. 5. Forward models of the restored cross-sections shown in Fig. 4c in which circular strain markers are included. (a) is the stage previous to normal fault development and (e) is the present-day stage. (b–d) represent intermediate stages.

layer-parallel shear is used (right column of Fig. 8). In 70° dipping antithetic and synthetic shear, vertical shear and layer-parallel shear, the maximum elongation dips toward the master fault; it dips gentler in antithetic shear than in vertical shear; it dips gentler in vertical shear than in synthetic shear; it dips slightly steeper in layer-parallel shear than in vertical shear.

Our analysis of a physical experiment and a natural example shows that 85° and 65° dipping antithetic shear respectively (5° and 25° shear angle) is the restoration/forward modelling algorithm that predicts the most reasonable results (Figs. 2 and 5). In addition, this algorithm yields satisfactory results irrespective of the amount of horizontal extension undergone by the structures. Our conclusions regarding the appropriate shear dip to model the experiment (85° dipping shear, that is, 5° shear angle) differ slightly from those of Dula (1991) since he estimated a shear dip around 70° (20° shear angle). However, the shear values obtained by Dula (1991) are derived from displacement paths in the most deformed region of the hangingwall, whereas our shear values correspond to an average of the whole hangingwall. Natural/experimental deformation is kinematically complex; however, a relatively simple algorithm that assumes a single dominant deformation mechanism appears to be adequate to model the rollover anticline developed in a clay experiment and in a natural listric normal fault. The small irregularities observed may be due to the assumption of a constant and uniform shear, which is an oversimplification of the complex process active during hangingwall deformation (Ellis and McClay, 1988; Dula, 1991; Mitra, 1993; Withjack et al., 1995; McClay, 1996), and probably to compaction not accounted for in our analysis.

The similarity between maps of incremental deformation and maps of deformation in the present-day section across the natural example is probably due to the smooth fault dip variations (a difference of less than 35° in dip from the steeper to the shallower part of the fault) and the small amount of horizontal extension (around 10%) which caused small offset along the fault (for instance, the top of the pre-growth beds was displaced only along the upper part of the fault ramp, which has an approximately constant dip). This suggests that in those cases where faults are non-planar but display a smooth geometry with no abrupt/large dip variations and/or the displacement along them is not large, sequential restorations/step-by-step forward modelling may not be essential to obtain reasonable deformation values, and this substantially simplifies the procedure and shortens the time employed.

In some previous methods of cross-section restoration, the strain was a necessary (e.g., Cloos, 1947; Oertel, 1974, 1980; Schwerdtner, 1977; Hossack, 1978; Oertel and Ernst, 1978; Cobbold, 1979; Cobbold and Percevault, 1983; Woodward et al., 1986; Ramsay and Huber, 1987; Protzman and Mitra, 1990; Gray and Willman, 1991; Howard, 1993; Mitra, 1994; Morgan et al., 1994; Kirkwood, 1995; Morgan and Karig, 1995; Flöttmann and James, 1997) or an optional (Wickham and Moeckel, 1997) input parameter to be incorporated into the restoration procedure at different points of the cross-section. In the approach used here the strain is a result (Figs. 5–7) rather than a required input, similarly to the methods presented by De Paor (1990), Allmendinger (1998),

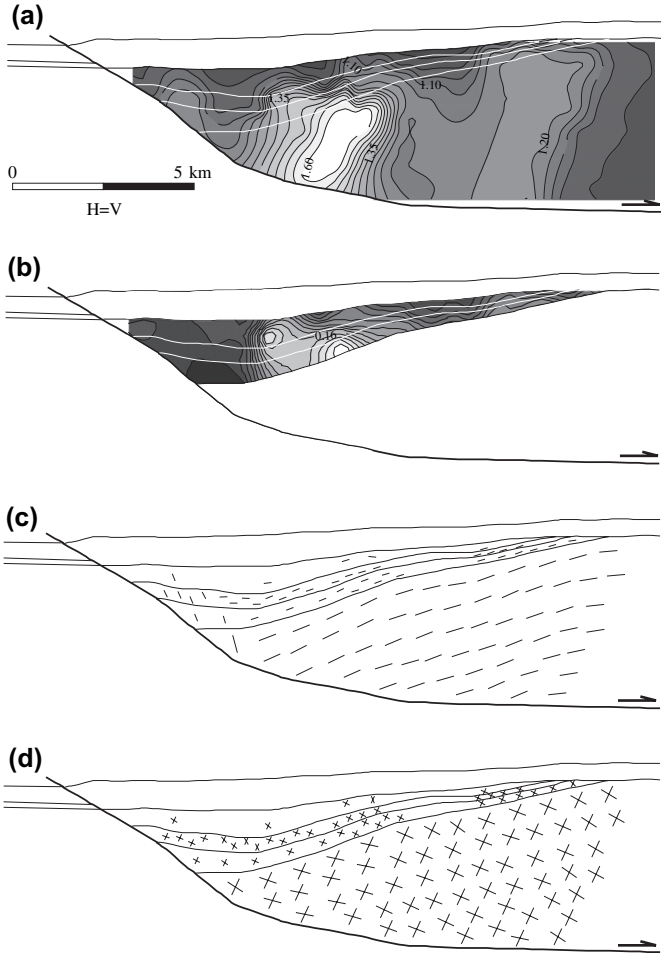

Fig. 6. Present-day section across the growth rollover anticline over a listric normal fault in the Central Sumatra Basin, Indonesia shown in Fig. 3 including (a) contours of ellipticity, (b) contours of layer parallel extension/contraction, (c) orientation of maximum elongation and (d) orientation of lines of no finite longitudinal strain. The maximum value of ellipticity is 1.60 (white areas) and the contour interval is 0.05. The contours of layer-parallel extension (positive values) indicate that bed length increased except for the left side of the cross-section, adjacent to the fault, where −0.02 values indicate that beds were shortened, being the maximum value 0.24 (white areas) and 0.02 the contour interval. Lines of maximum elongation and lines no finite longitudinal strain are not shown in some portions of the three Oligocene growth beds indicating that the strain measured in these areas is almost negligible.

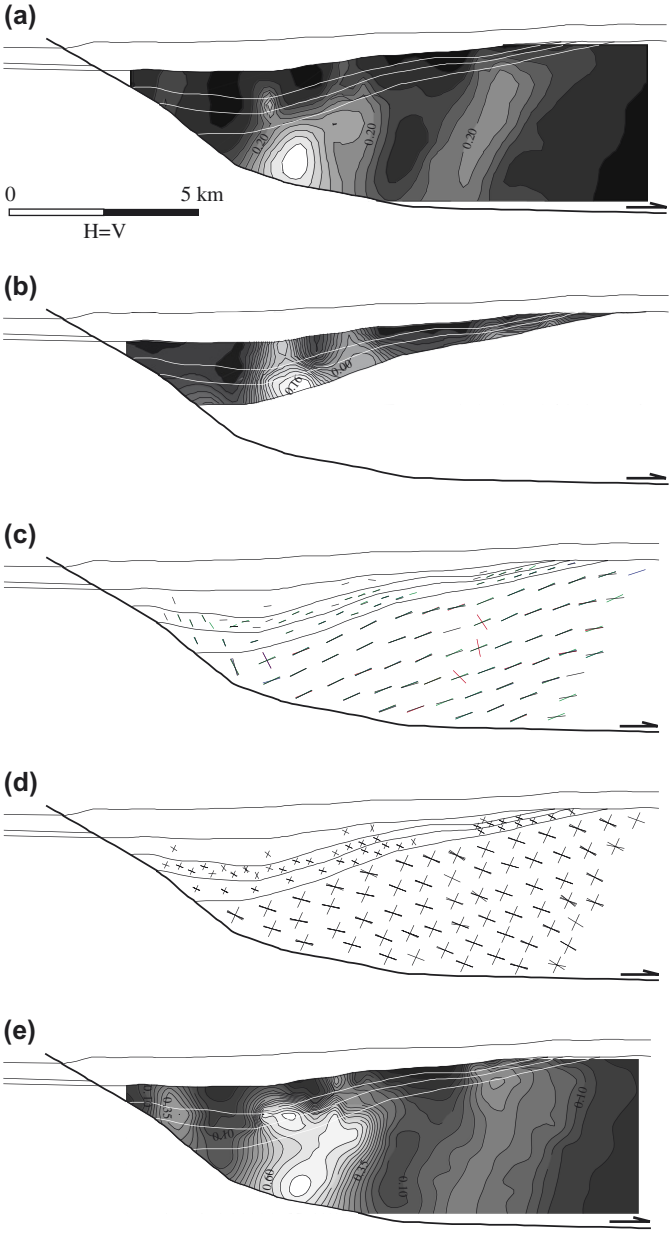

Fig. 7. Present-day section across the growth rollover anticline over a listric normal fault in the Central Sumatra Basin, Indonesia shown in Fig. 3 including (a) contours of incremental ellipticity, (b) contours of incremental layer parallel extension/contraction, (c) orientation of maximum elongation for all the growth stages, (d) orientation of lines of no finite longitudinal strain for all the growth stages, and (e) contours of velocity of ellipticity variation. The maximum value of incremental ellipticity is 0.25 (white areas) and the contour interval is 0.01. The maximum value of layer-parallel extension/contraction is 0.16 (white areas) and the contour interval is 0.02. The maximum value of velocity of ellipticity variation is 0.75 (white areas) and the contour interval is 0.05. Lines of maximum elongation and lines no finite longitudinal strain are not shown in some portions of the three Oligocene growth beds, indicating that the strain measured in these areas is almost negligible.

Erickson et al. (2000) Rouby et al. (2000), Dunbar and Cook (2003) and Sanders et al. (2004). Thus, in addition to validating interpretations of structures by deciphering the original geometry and position of beds and structures, quantifying the amount of contraction/extension, etc., cross-section restoration combined with forward modelling provides a valuable tool to predict the distribution of internal deformation throughout folded/faulted rocks.

The approach employed can only predict a bulk kinematic description of the strain path by which the structures arrived at their present configuration and does not decipher processes, types and orientations of second-order structures that may accommodate the deformation predicted by the strain markers because equivalent strains may be accommodated by subsidiary faults of varying orientations and displacements (e.g., Dula, 1991; Hauge and Gray, 1996). The displacement along listric normal faults and formation of rollover anticlines may involve ductile structures if weak units are present (Dula, 1991; Withjack et al., 1995), or slip along bedding surfaces,

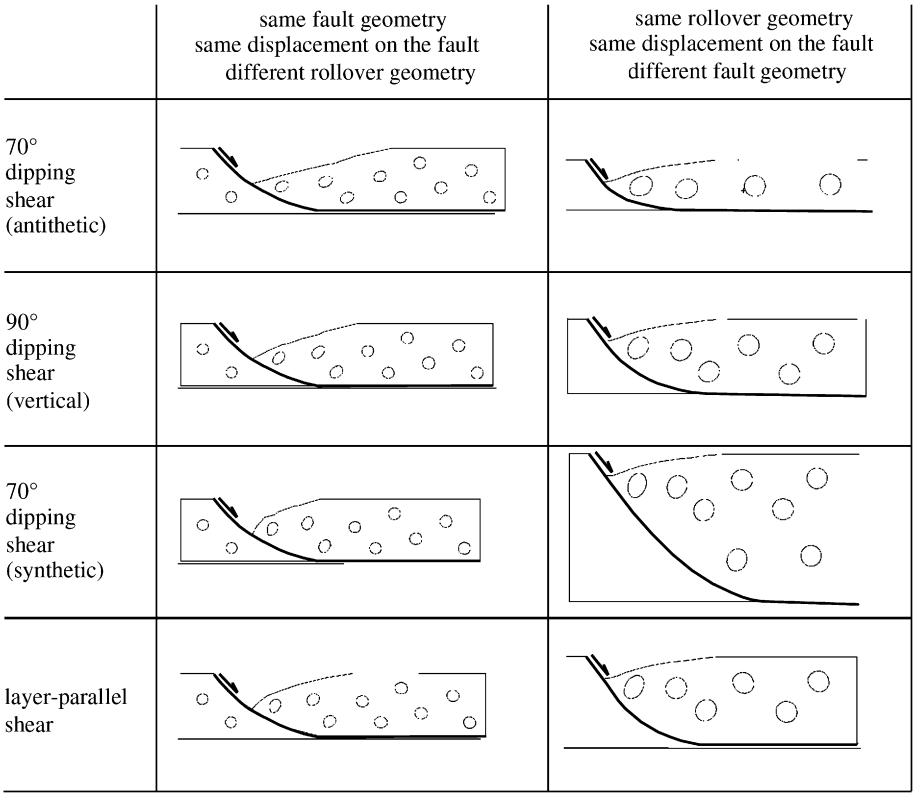

Fig. 8. Retro-deformable sections across theoretical rollover anticlines over listric normal faults including strain markers. The left column shows different rollovers over the same fault with the same displacement on the fault modelled using various algorithms, whereas the right column shows the same rollover with the same displacement on the fault over different faults modelled using various algorithms.

antithetic/synthetic secondary faults, rotated rigid fault blocks, pervasive joints and tensional veins, etc. with a wide range of orientations if more competent units occur (e.g., Higgs et al., 1991; Muñoz et al., 1994; Hauge and Gray, 1996). The features of the structures that accommodate natural deformations depend on many factors and predicting them demands a mechanical approach (see Maerten and Maerten, 2006 for a review of these techniques) rather than a kinematical one. Nevertheless, if competent rocks are involved in the structure and deformation is to be accommodated by fracturing, the analysis of the strain markers may supply some clues on fracture orientation and distribution. Thus, open fractures are likely to develop perpendicular to the maximum extension axis of the strain ellipses. Shear planes often occur along one set of lines of no finite longitudinal strain (e.g., White et al., 1986; Allmendinger, 1998), whereas the second set of lines, synthetic to the master fault, may not correspond to fracture planes and may rotate passively during deformation (Allmendinger, 1998; Allmendinger et al., 2004). It is likely that areas with greater strain correspond to more bed damage, and possibly more intense fracturing (e.g., Sanders et al., 2004). Since the higher the strain rate, the more likely for rocks to behave in a brittle manner, high deformation velocities may indicate high fracture intensity. High values of layer parallel strain indicate areas where the main rock anisotropy, namely bedding, was pervasively extended. It is likely that these regions will have more fractures, higher displacement along fractures and/or fractures will be developed at a smaller angle to bedding.

The approach used to predict strains has some advantages over other predictive techniques. For instance, using several algorithms until the best restoration is obtained ensures that the modelling algorithm employed to predict the strains is the most appropriate. Unlike forward modelling techniques, that evaluate the appropriateness of the modelling algorithms and input parameters by how well they deform beds, the method used here assesses the modelling algorithms by how well they restore beds. Checking that deformation has been properly removed from a cross-section and that the resulting restored section is geologically reasonable is usually easier than checking the resemblance between forward models and true deformed structures. Unfortunately, the strains predicted are not totally reliable because they may include errors that depend on the quality of the geological/geophysical data and ability of the interpreter to choose a correct line of section, to construct the geological section, to place appropriate pin and loose lines, and to select a suitable restoration algorithm. Another drawback that may be responsible for deviations from the true strain of the structure is that plane strain is assumed.

6. Conclusions

The approach employed here based on cross-section restoration and kinematic forward modelling successfully predicted

internal deformation of 2D sections across geological bodies, accurately modelled the strain of a physical experiment, and defined strain that was beyond the resolution of seismic data in the case of a subsurface structure. Restoration algorithms that produce reasonable geometry of beds and pin/loose lines before deformation, remove the displacement along faults, and give reasonable amounts of contraction/extension are also able to predict the strain undergone by the rocks when employed to forward model the structures. The technique, successfully applied to rollover anticlines over listric normal faults, may be used for any type of contractional, extensional, reactivated, etc. structure as long as correct algorithms for each particular case are employed.

The modelling technique provides insight into the internal deformation of structures and may be used to refine structural interpretations. This is particularly important from the purely scientific point of view and when the geometry and distribution of potential geological resources have structural controls. Even if the procedure used can only predict the broad orientation and distribution of fractures, if strain is accommodated by brittle structures this technique is a useful tool because it may help to define compartmentalization, highly damaged areas, porosity and fluid migration paths, and therefore, the choice of optimal strategies for exploration and production in fractured hydrocarbon reservoirs, mineral deposits and aquifers, emplacement of underground waste disposal and fluids storage, etc.

The simple technique used models the complex process of internal deformation in folded regions related to faulting. It is possible to develop more complex algorithms to improve the results; however, complex models require multiple input parameters, which are unknown in many cases, and the predictive capabilities of the methods become substantially reduced. We believe that this approach successfully predicts the strain architecture in folded/faulted regions and requires few input parameters which are usually available. To gain a better understanding of strain in these settings and to reach more solid conclusions it would be necessary to test physical experiments and natural examples including listric normal faults at various scales, with various shapes, with several amounts of horizontal extension, offsetting different materials, including footwall deformation and subsidiary faults, etc.

Acknowledgements

We acknowledge financial support by projects CGL2005-02233/BTE (3D modelling of folding kinematic mechanisms), CGL2006-12415-C03-02/BTE (structural evolution of the Central Andes between parallels 23° and 33° during the Upper Paleozoic) and CSD2006-0041 (Topo-Iberia) under Consolider-Ingenio 2010 Programme funded by the Spanish Ministry for Education and Science. Comments by Jesús Aller, Fernando Bastida, Thomas G. Blenkinsop, Russell K. Davies, Richard G. Gibson, Rick H. Groshong, Laurent Maerten and Sandro Serra substantially improved the initial version of the manuscript. Carlos Salvador, Isidro Ibáñez and Gabriel Gutiérrez-Alonso supplied us with software to interpolate and contour the strain parameters. Robert Bond and Oscar Fernández provided us with useful references.

References

Allmendinger, R.W., 1998. Inverse and forward numerical modelling of trishear fault-propagation folds. Tectonics 17, 640–656.

Allmendinger, R.W., Zapata, T., Manceda, R., Dzelalija, F., 2004. Trishear kinematic modelling of structures, with examples from the Neuquén Basin, Argentina. In: McClay, K.R. (Ed.), Thrust Tectonics and Hydrocarbon Systems, 82. American Association of Petroleum Geologists Memoir, pp. 356–371.

Bastida, F., Bobillo-Ares, N.C., Aller, J., Toimil, N.C., 2003. Analysis of folding by superposition of strain patterns. Journal of Structural Geology 25, 1121–1139.

Bulnes, M., McClay, K., 1999. Benefits and limitations of different 2D algorithms used in cross section restoration of inverted extensional faults: application to physical experiments. Tectonophysics 312, 175–189.

Bulnes, M., Poblet, J., 1999. Estimating the detachment depth in cross sections involving detachment folds. Geological Magazine 136, 395–412.

Cloos, E., 1947. Oolite deformation in the South Mountain Fold, Maryland. Geological Society of America Bulletin 58, 843–918.

Cobbold, P.R., 1979. Removal of finite deformation using strain trajectories. Journal of Structural Geology 1, 67–72.

Cobbold, P.R., Percevault, M.N., 1983. Spatial integration of strains using finite elements. Journal of Structural Geology 5, 299–305.

De Paor, D.G., 1990. Cross-section balancing in space and time. In: Letouzey, J. (Ed.), Petroleum Tectonics in Mobile Belts. J. Letouzey and Editions Technip, Paris, pp. 149–154.

Dula, W.F., 1991. Geometric models of listric normal faults and rollover folds. American Association of Petroleum Geologists Bulletin 75, 1609–1625.

Dunbar, J.A., Cook, R.W., 2003. Palinspastic reconstruction of structure maps: an automated finite element approach with heterogeneous strain. Journal of Structural Geology 25, 1021–1036.

Ellis, P.G., McClay, K., 1988. Listric extensional fault systems—results of analogue model experiments. Basin Research 1, 55–70.

Erickson, S.G., Hardy, S., Suppe, J., 2000. Sequential restoration and unstraining of structural cross sections: applications to extensional tectonics. American Association of Petroleum Geologists Bulletin 84, 234–249.

Flöttmann, T., James, J., 1997. Influence of basin architecture on the style of inversion and fold-thrust belt tectonics - the southern Adelaide Fold-Thrust Belt, South Australia. Journal of Structural Geology 19, 1093–1110.

Gray, D.R., Willman, C.E., 1991. Thrust-related strain gradients and thrusting mechanisms in a chevron folded sequence, southeastern Australia. Journal of Structural Geology 13, 691–710.

Hauge, T.A., Gray, G.G., 1996. A critique of techniques for modelling normal-fault and rollover geometries. In: Buchanan, P.G., Nieuwland, D.A. (Eds.), Modern Developments in Structural Interpretation, Validation and Modelling. Geological Society Special Publication, 99, pp. 89–97.

Higgs, W.H., Williams, G.D., Powell, C.M., 1991. Evidence for flexural shear folding associated with extensional faults. Geological Society of America Bulletin 103, 710–717.

Hossack, J.R., 1978. The correction of stratigraphic sections for tectonic finite strain in the Bygdin area, Norway. Journal of the Geological Society 135, 229–241.

Howard, J.H., 1993. Restoration of cross sections through unfaulted, variable strained data. Journal of Structural Geology 15, 1331–1342.

Kirkwood, D., 1995. Strain partitioning and progressive deformation history in a transpressive belt, northern Appalachians. Tectonophysics 241, 15–34.

Lisle, R.J., 1994. Detection of zones of abnormal strains in structures using Gaussian curvature analysis. American Association of Petroleum Geologists Bulletin 78, 1811–1819.

Maerten, L., Maerten, F., 2006. Chronologic modeling of faulted and fractured reservoirs using geomechanically based restoration: technique and industry applications. American Association of Petroleum Geologists Bulletin 90, 1201–1226.

Masaferro, J.L., Bulnes, M., Poblet, J., Eberli, G.P., 2002. Episodic fold uplift inferred from the geometry of syntectonic carbonate sedimentation: the Santaren anticline, Bahamas foreland. Sedimentary Geology 146, 11–24.

McClay, K.R., 1996. Recent advances in analogue modelling: Uses in section construction and validation. In: Buchanan, P.G., Nieuwland, D.A. (Eds.), Modern Developments in Structural Interpretation, Validation and Modelling. Geological Society Special Publication, 99, pp. 201–225.

Mitra, S., 1993. Geometry and kinematic evolution of inversion structures. Geological Society of America Bulletin 77, 1159–1191.

Mitra, G., 1994. Strain variation in thrust sheets across the Sevier fold and thrust belt (Idaho-Utah-Wyoming): implications for section restoration and wedge taper evolution. Journal of Structural Geology 16, 585–602.

Morgan, J.K., Karig, D.E., 1995. Kinematics and a balanced and restored cross-section across the toe of the eastern Nankai accretionary prism. Journal of Structural Geology 17, 31–45.

Morgan, J.K., Karig, D.E., Maniatty, A., 1994. The estimation of diffuse strains in the toe of the western Nankai accretionary prism: a kinematic approach. Journal of Geophysical Research 99, 7019–7032.

Muñoz, J.A., McClay, K., Poblet, J., 1994. Synchronous extension and contraction in frontal thrust sheets of the Spanish Pyrenees. Geology 22, 921–924.

Oertel, G., 1974. Unfolding of an antiform by the reversal of observed strains. Geological Society of America Bulletin 85, 445–450.

Oertel, G., 1980. Strain in ductile rocks on the convex side of a folded competent bed. Tectonophysics 66, 15–34.

Oertel, G., Ernst, W.G., 1978. Strain and rotation in a multilayered fold. Tectonophysics 48, 77–106.

Ormand, C.J., Hudleston, P.J., 2003. Strain paths of three small folds from the Appalachian Valley and Ridge, Maryland. Journal of Structural Geology 25, 1841–1854.

Poblet, J., Bulnes, M., 2005a. Fault-slip, bed-length and area variations in experimental simple rollover anticlines over listric normal faults: influence in extension and depth to detachment estimations. Tectonophysics 396, 97–117.

Poblet, J., Bulnes, M., 2005b. Estimating extension and depth to detachment in simple rollover anticlines over listric normal faults. Trabajos de Geología 25, 85–102.

Protzman, G.M., Mitra, G., 1990. Strain fabric associated with the Meade thrust sheet: implications for cross-section balancing. Journal of Structural Geology 12, 403–417.

Ramsay, J.G., Huber, M.I., 1987. The Techniques of Modern Structural Geology. In: Folds and Fractures, Vol. 2. Academic Press, London.

Roberts, A., 2001. Curvature attributes and their application to 3D interpreted horizons. First Break 19, 391–412.

Rouby, D., Xiao, H., Suppe, J., 2000. 3-D restoration of complexly folded and faulted surfaces using multiple unfolding mechanisms. American Association of Petroleum Geologists Bulletin 84, 805–829.

Samson, P., Mallet, J.M., 1997. Curvature analysis of triangulated surfaces in structural geology. Mathematical Geology 29, 391–412.

Sanders, C., Bonora, M., Richards, D., Kozlowski, E., Sylwan, C., Cohen, M., 2004. Kinematic structural restorations and discrete fracture modeling of a thrust trap: a case study from the Tarija Basin, Argentina. Marine and Petroleum Geology 21, 845–855.

Sanderson, D.J., 1982. Models of strain variation in nappes and thrust sheets: a review. Tectonophysics 88, 201–233.

Schwerdtner, W.M., 1977. Geometric interpretation of regional strain analyses. Tectonophysics 39, 515–531.

Shaw, J.H., Hook, S.D., Sitohang, E.P., 1997. Extensional fault-bend folding and synrift deposition: an example from the Central Sumatra Basin, Indonesia. American Association of Petroleum Geologists Bulletin 81, 367–379.

Thorbjornsen, K.L., Dunne, W.M., 1997. Origin of a thrust-related fold: geometric vs kinematic tests. Journal of Structural Geology 19, 303–319.

White, N., Jackson, J.A., McKenzie, D.P., 1986. The relationships between the geometry of normal faults and that of the sedimentary layers in their hanging walls. Journal of Structural Geology 8, 897–909.

Wickham, J., Moeckel, G., 1997. Restoration of structural cross sections. Journal of Structural Geology 19, 975–986.

Withjack, M.O., Islam, Q.T., La Pointe, P.R., 1995. Normal faults and their hangingwall deformation: an experimental study. American Association of Petroleum Geologists Bulletin 79, 1–18.

Woodward, N.B., Gray, D.R., Spears, D.B., 1986. Including strain data in balanced cross sections. Journal of Structural Geology 8, 313–324.